Commissioning of the prototype stripline BPM system for the CLIC Drive Beam

A. Benot-Morell*
CERN, Geneva, Switzerland, and IFIC (CSIC-UV), Valencia, Spain

B.P. Bielawski, D. Gudkov, F. Locci, S. Magnoni, L. Søby, and M. Wendt
CERN, Geneva, Switzerland

A. Faus-Golfe
IFIC (CSIC-UV), Valencia, Spain

J.M. Nappa and S. Vilalte
IN2P3-LAPP, Annecy-le-Vieux, France

S. Smith
SLAC, Menlo Park, California, USA
(Dated: October 15, 2015)

In collaboration with SLAC, LAPP and IFIC, a first prototype of a stripline Beam Position Monitor (BPM) for the CLIC Drive Beam and its associated readout electronics has been successfully tested in the Test Beam Line of the CLIC Test Facility 3 (CTF3) at CERN. In addition, a modified prototype with downstream terminated electrodes has been developed to improve the suppression of unwanted RF signal interference and installed in the CLIC Two-Beam Module (TBM). This paper presents measurements and performance of this BPM system with different CTF3 beam configurations and compares the results with laboratory measurements and electromagnetic simulations.

PACS numbers: 07.50.-e, 29.20.Ej, 29.27.Fh, 84.40.Az

I. INTRODUCTION

CLIC, a Compact electron-positron LInear Collider proposed to probe high energy physics (HEP) in the TeV energy scale, is based on a two-beam scheme. RF power, required to accelerate a high energy luminosity beam is extracted from a high current Drive Beam (DB), whose decelerator requires more than 40000 quadrupoles, each holding a BPM. These BPMs face several challenges, as they will operate in close proximity to the Power Extraction and Transfer Structures (PETS), with demanding accuracy and resolution requirements (20 μm and 2 μm, respectively) [1]. They have to be compact, inexpensive and operate below the waveguide (WG) cut-off frequency of the beam pipe to ensure purity of the position signals, which rules out the signal processing at the 12 GHz bunching frequency. Also wakefields, and hence the longitudinal impedance, should be kept low. The first proposed solution was a compact, downstream shortened stripline BPM utilizing a low-frequency (< 40 MHz) signal processing scheme operating in the accelerator tunnel [2]. The system has been recently tested with beam in the CLIC Test Facility 3 (CTF3) [3], in presence of low and high power interfering 12 GHz RF signals from the PETS. In parallel, a second prototype stripline BPM with improved notch-filtering properties at 12 GHz has been developed and installed in the CLIC Two-Beam Module (TBM) [4, 5].

* alfonso.benot.morell@cern.ch

II. SYSTEM DESIGN

The first prototype stripline BPM pickup is compact (with downstream short-circuited electrodes) and fits into the adjacent quadrupole vacuum chamber. Each of the four electrodes spans an angular coverage of 45° and has a characteristic impedance of 50 Ω. The magnitude of the transfer function of a stripline pickup is the absolute value of a sine wave with periodic notches given by:

$$f_{z_N} = N \cdot \frac{c}{2L} \tag{1}$$

where $N \in \mathbb{N}^+$, L is the electrode length and c is the speed of light in vacuum. By choosing the appropriate value of L it is possible to tune the $\mathrm{N^{th}}$ non-DC notch to the frequency of the interference produced by the high power accelerating structures (PETS): 12 GHz, which is also the beam bunch frequency. Therefore, in the time domain, the idealized response to a multi-bunch beam only shows the N first and the N last bunches, all other bunches in-between are cancelled. Fig. 1 shows this effect for $N = 2$, chosen for the design as it gives the minimum feasible electrode length among the possible values, $L =$ 25 mm. Other relevant design parameters are listed in Table I.

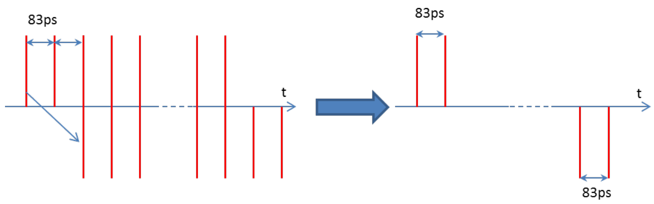

FIG. 1. Time response of the compact prototype stripline BPM PU to a multi-bunch beam.

TABLE I. Parameters of the compact prototype stripline BPM for the CLIC Drive Beam.

Parameter	Value	Comment
Diameter	24 mm	stripline ID
Stripline length	25 mm	
Width	12.5 %	of circumference (45°)
Characteristic impedance	50 Ω	
Duct aperture	23 mm	
Resolution	2 μm	Full train
Accuracy	20 μm	
Time resolution	10 ns	BW > 20 MHz

A strong resonance peak of the transverse wake impedance of the device was observed around 12 GHz in simulations [2]. A ring of SiC RF damping material was placed at the downstream end of the electrodes (Fig. 2) to absorb this and other higher-order modes (HOMs).

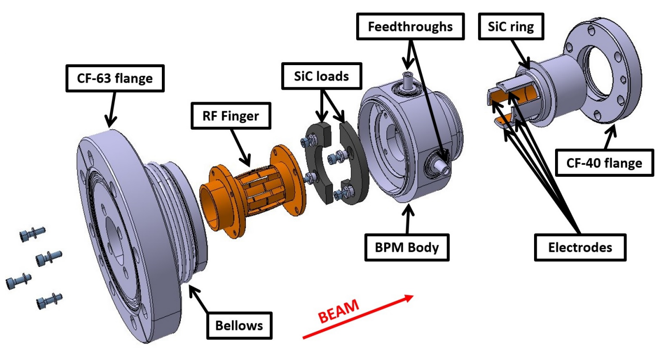

FIG. 2. Assembly view of the compact stripline BPM prototype for the CLIC Drive Beam.

The signal processing will be performed at baseband frequencies ranging 4 to 40 MHz, to avoid non-local confounding signals, mainly coming from the PETS, starting at 7.6 GHz, the cut-off frequency of the TE_{11} mode for a circular waveguide of 23mm pipe aperture. An analog shaping circuit, mainly an integration/low-pass filtering, is needed to perform a correct acquisition of the electrode signals, since the pulses at the output signal of the pickup are expected to be very intense and narrow in the presence of a beam with a 242 ns train of bunches and 10 ps bunch length. The resulting electrode signal should reflect beam position and intensity during the passage of a multi-bunch train, but should return to zero in time to allow acquisition of the next train. The combination of filters found in simulations to perform an optimal shaping is the following: a 4 MHz first-order low-pass filter, a 20 MHz first-order low-pass filter and a 35 MHz second-order low-pass filter (Fig. 3). A programmable attenuator has been included in order to adapt the signals produced by all possible CLIC Drive Beam configurations (Fig. 4) to the input range of the ADC. A thorough description of the readout electronics and further details of the design can be found in [6].

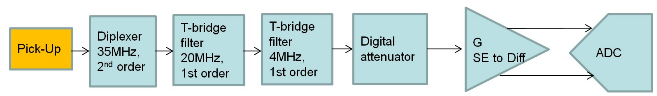

FIG. 3. Block diagram of the analog readout electronics.

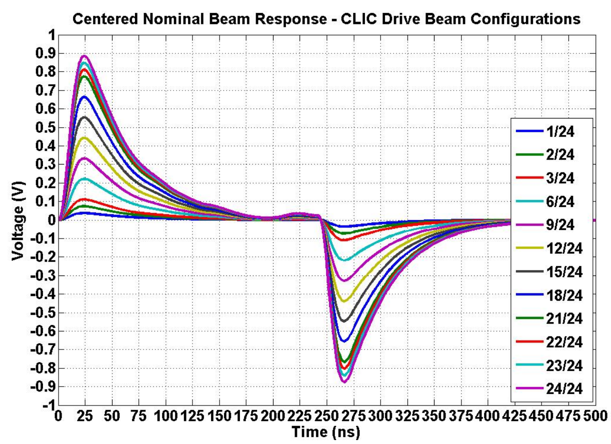

FIG. 4. Simulated output signals of the filtering stage for different CLIC Drive Beam configurations (centered beams).

The beam position in the horizontal, x, and vertical, y, planes can be estimated using difference-over-sum processing [7] as:

$$x, y = \frac{R}{2} \cdot \left(\frac{\Delta}{\Sigma}\right)_{H,V} \tag{2}$$

where R is the beam pipe radius, Δ the difference and Σ the sum of the opposite electrode signals for each plane. The area defined by the second lobe of the output signals (Fig. 4) has been used as metrics for the position calculation for all tests presented in this paper. The difference-over-sum ratio has been obtained as:

$$\frac{\Delta}{\Sigma} = \frac{S^+ - S^-}{S^+ + S^-} \tag{3}$$

where S^+ and S^- are the surface values under the second lobe of the signals from the positive and the negative channels, respectively, of each plane.

III. LABORATORY CHARACTERIZATION

A. Position characteristics and linearity

The linearity and sensitivity parameters are given, for each plane, by:

$$x, y \; = \; (S_{H,V}^{-1}) \cdot \left(\frac{\Delta}{\Sigma}\right)_{H,V} + EOS_{H,V} \qquad (4)$$

where $S_{H,V}$ is the sensitivity and $EOS_{H,V}$ is the electrical offset. Another parameter to study is $\sigma_{H,V}$, the RMS value of the linearity error for each plane giving the uncertainty in the position measurements.

The position characteristics for the full system was measured using a stretched wire fed by an RF excitation signal while being moved in 1 mm steps in the range ± 6 mm. The output waveforms when the wire is centered are shown in Fig. 5. The measured sensitivity curves and the one obtained by electromagnetic simulation ($y = 0$ in Fig. 6) are compared in Fig. 7 for the vertical and the horizontal planes. Table II shows the values for the position sensitivity at the origin, the electrical offset and the RMS linearity error for both planes. Although the performance of the electronics was satisfactory, showing the expected signal shape and levels [6], the obtained position sensitivity at the origin was lower than estimated by the linear approximation in Eq. (2), 166.67 m^{-1}, but closer to the result obtained by electromagnetic simulation for the horizontal plane): 137.01 m^{-1}. Charge accumulation and impedance mismatches in the measurement setup are the most likely causes of this difference in sensitivity values.

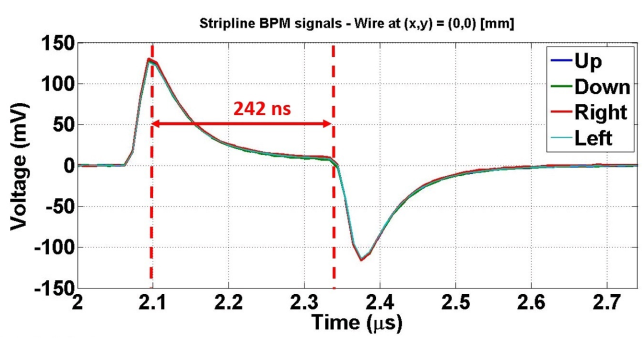

FIG. 5. Output waveforms of the electronics produced by the low-frequency emulation of a centered 242 ns multi-bunch beam in laboratory.

B. Transfer function measurement

The transfer function of the BPM was analysed with a coaxial transmission-line setup [8]. An inner rod, traversing the BPM, serves as center conductor of the coaxial

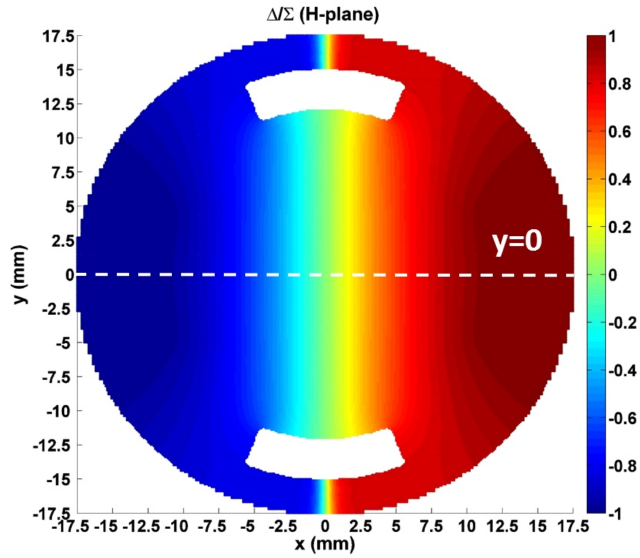

FIG. 6. Simulated difference-over-sum ratio in the cross-section of the compact prototype stripline BPM for the horizontal plane.

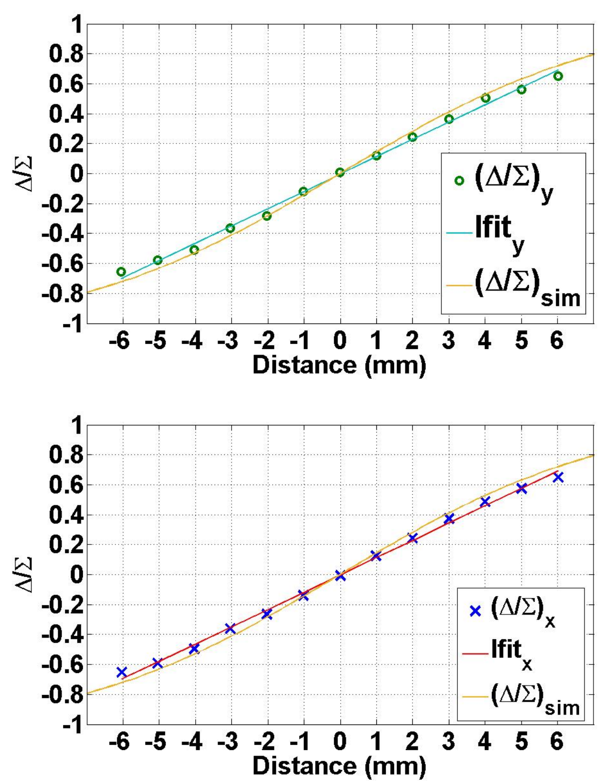

FIG. 7. Simulated (orange trace) and measured (green trace) sensitivity curves in laboratory in the vertical (top) and the horizontal (bottom) planes for the compact prototype stripline BPM.

structure, which has conical transitions towards the SMA connectors at both ends, providing a constant character-

TABLE II. Linearity and sensitivity parameters for the vertical (top) and horizontal (bottom) planes.

Parameter	Measurement	Theory	Simulation
	Vertical		
S_V [m^{-1}]	115.19 ± 2.32	166.67	137.01
EOS_V [mm]	0.03 ± 0.08	0.00	0.00
σ_V [μm]	251.07		
	Horizontal		
S_H [m^{-1}]	115.17 ± 1.98	166.67	137.01
EOS_H [m]	0.02 ± 0.07	0.00	0.00
σ_H [μm]	214.07		

istic impedance of 50 Ω. A sine wave stimulus signal was swept in the range 0.003-20 GHz to measure the magnitude of the transfer function (Fig. 8). We observed major differences between measured and ideal (theoretical) transfer functions, e.g. that the two first minima, which should be located at 6 GHz and 12 GHz, have been displaced to lower frequencies due to the inclusion of the SiC ring [9], 4.48 GHz and 7.34 GHz, respectively, which hints to an effective electrical length of 33.5 mm instead of the desired 25 mm. In addition, all the sine lobes of the stripline transfer function from the second one are distorted, pointing to high-order effects on the BPM. These two factors result in an extremely poor rejection of the PETS interference at 12 GHz, of about 4 dB (green trace) instead of the theoretically expected 40 dB (blue trace).

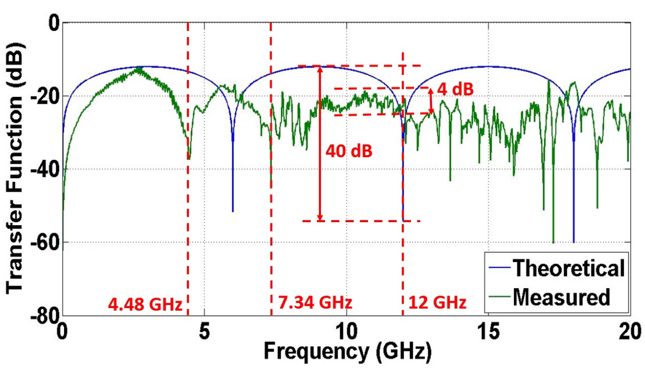

FIG. 8. Theoretical (blue trace) and measured (green trace) transfer function of the compact prototype stripline BPM.

IV. BEAM TESTS AT CTF3

Following its comprehensive laboratory characterization, the prototype stripline BPM with short-circuited electrodes at their downstream end was tested under realistic beam conditions in CTF3. The BPM pickup was installed in the Test Beam Line (TBL) [10], a scaled version and proof of concept of the CLIC Drive Beam decelerator. In order to study the immunity of the device to high power RF pulses, it was installed as close as possible to the last PETS in TBL (Fig. 9): at position 0860, downstream of an inductive BPM (position 0850) and upstream of an F-type quadrupole (position 0900). Two types of tests were performed: linearity/sensitivity parameters and resolution.

A. Linearity and sensitivity

The goal of this test was to study the behavior of the BPM and the influence of the interfering signals coming from the PETS at the beam bunching frequency (12 GHz) on the position measurement. For this purpose, the test was conducted using two different beam configurations: high and low current, corresponding to high and low extracted PETS power values at 12 GHz, respectively.

In order to evaluate the linearity and sensitivity parameters of the prototype, the F-type quadrupole at position 0800 was moved in both the horizontal and the vertical planes, so that the induced beam displacements could be observed at position 0860. The beam was steered in a range of approximately ±5 mm for each plane, displacing the F-type quadrupole at position 0800. The mover at position 0805 was used as actuator. The reading provided by the neighboring TBL inductive BPMs [11] at positions 0850 and 0910 was used as reference for the calculation of the expected positions.

1. *Installation with 45°-rotated electrodes*

In a first test, the compact prototype stripline BPM was installed under a 45° rotation for mechanical considerations. Under these conditions, the position characteristics differs from the one considered in section III due to the new location of the electrodes with respect to the beam movement axes. While the approximation in Eq. (2) still applies, the difference-over-sum ratio in this situation can be calculated as:

$$\left(\frac{\Delta}{\Sigma}\right)_V = \frac{(S_{UL}+S_{UR})-(S_{DL}+S_{DR})}{S_{UR}+S_{DR}+S_{UL}+S_{DL}} \qquad (5)$$

for the vertical plane and as:

$$\left(\frac{\Delta}{\Sigma}\right)_H = \frac{(S_{UR}+S_{DR})-(S_{UL}+S_{DL})}{S_{UR}+S_{DR}+S_{UL}+S_{DL}} \qquad (6)$$

for the horizontal plane, where R is the beam pipe radius and S_i, $i=(UR,UL,DL,DR)$ are the metrics from the i^{th} electrode used for the position calculation: we use again the surface values under the second lobe of the signals. An electromagnetic simulation of this test scenario (Fig.10) gives an estimated position sensitivity around the origin of 101.8 m^{-1}.

The CTF3 beam conditions at the time of this test provided beam current values of 10 A (6 MW of extracted

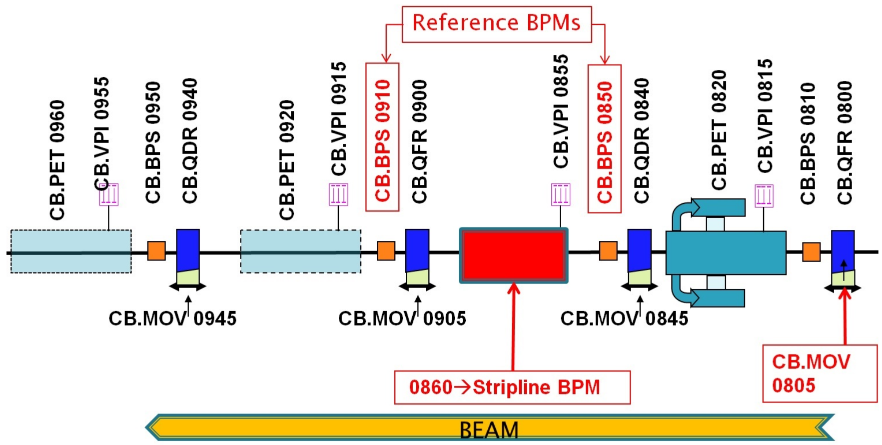

FIG. 9. Diagram of the TBL cells around the installation location for the prototype stripline BPM with short-circuited electrodes.

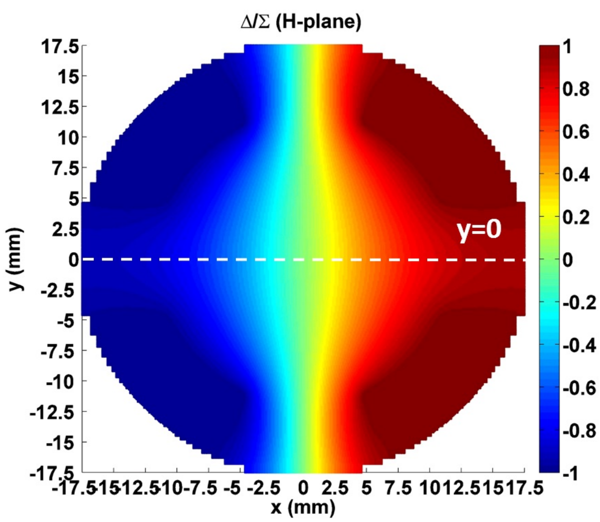

FIG. 10. Simulated difference-over-sum ratio in the cross-section of the compact prototype stripline BPM for the horizontal plane in a 45°-rotated installation.

PETS power) for the low current configuration and 22 A (60 MW of extracted PETS power). Table III summarizes, for both configurations, the results based on linear fit (Eq. 4) to obtain the sensitivity ($S_{V,H}$), the electrical offset ($EOS_{V,H}$) and the RMS linearity error. Figure 11 displays the measured data along with linear fits, showing the change in the electrical offset for the two power settings.

The measured sensitivities for each plane (Table III) experience a ±4% variation upon the increase of the extracted PETS RF power from 6 to 60 MW. The measured horizontal sensitivity values remain close to the simulated value of 101.8 m^{-1}, while the vertical sensitivity was found systematically lower. A possible reason for this result could be the presence of an active F-type quadrupole at position 0900, between the two reference

TABLE III. Measured linearity and sensitivity parameters of the prototype stripline BPM for both high- and low-power test configurations in the installation with 45°-rotated electrodes.

Parameter	Meas. LP	Meas. HP	Theory	Simulation
		Vertical		
S_V [m^{-1}]	72.4 ± 1.8	75.3 ± 0.6	117.9	101.8
EOS_V [mm]	-1.76 ± 0.07	-1.91 ± 0.02	0.00	0.00
σ_V [μm]	250.42	92.73		
		Horizontal		
S_H [m^{-1}]	98.1 ± 1.7	94.2 ± 1.4	117.9	101.8
EOS_H [mm]	0.24 ± 0.05	-0.46 ± 0.04	0.00	0.00
σ_H [μm]	182.87	120.00		

BPMs used for this test, located at positions 0850 and 0910. F-type quadrupoles focus the beam in the horizontal plane, defocussing it in the vertical one. This could affect the vertical position reading of the downstream reference BPM (0910), and therefore the calculated value of the expected vertical position. In order to avoid this effect, another test was attempted switching off the quadrupole, not being possible to operate in these conditions without losing the beam.

A decrease in the electrical offset was observed in the high-power test configuration for the coordinate not being swept (Figure 11). In addition, for this coordinate in both the high- and low-power test configurations, a tilt was observed, of 5 mrad for the horizontal plane and 7 mrad for the vertical one.

2. *Installation with axis-oriented electrodes*

A second test was performed after aligning the electrodes of the compact prototype stripline BPM with the x, y movement axes of the beam. The CTF3 beam conditions at the time of this test provided beam current values of 3.5 A (2.4 MW of extracted PETS power) for the

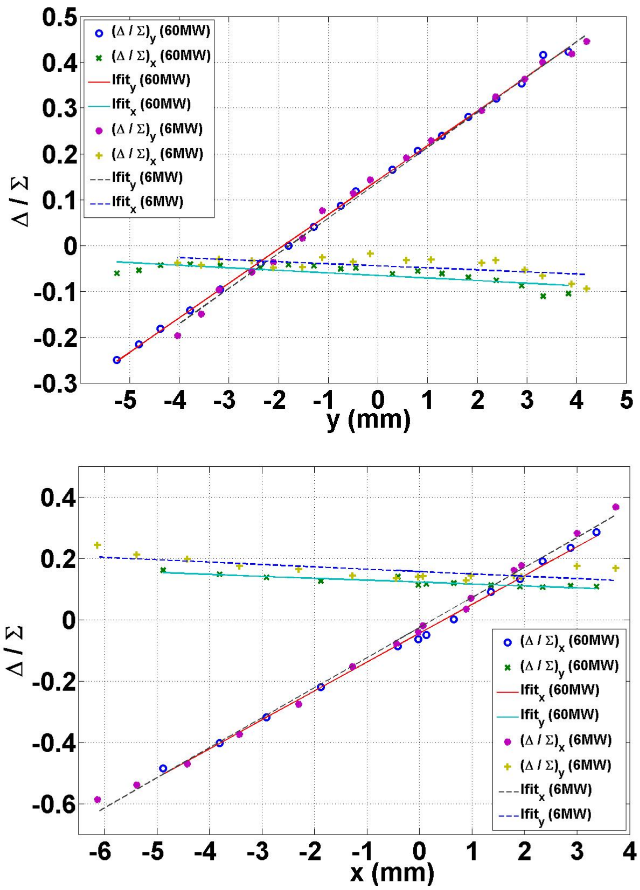

FIG. 11. Dependency of the difference-over-sum ratio on the beam displacement in the vertical (top) and horizontal (bottom) planes for extracted PETS RF power values of 6 MW (dashed lines) and 60 MW (solid lines) for the stripline BPM installation with 45-rotated electrodes.

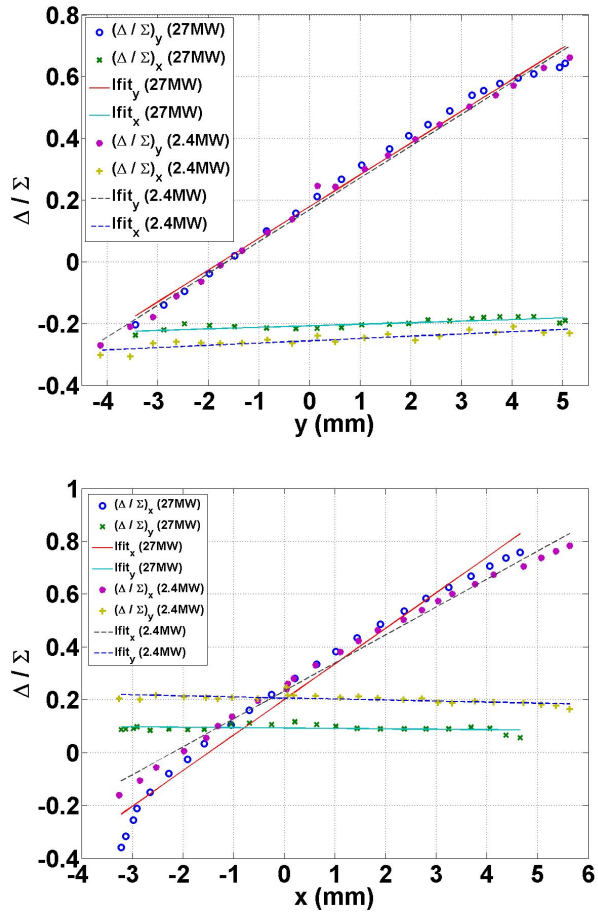

FIG. 12. Dependency of the difference-over-sum ratio on the beam displacement in the vertical (top) and horizontal (bottom) planes for extracted PETS RF power values of 2.4 MW (dashed lines) and 27 MW (solid lines) for the stripline BPM installation with axis-oriented electrodes.

low current configuration and 12 A (27 MW of extracted PETS power). Table IV summarizes, for both configurations, the results based on linear fit (Eq. 4) to obtain the sensitivity ($S_{V,H}$), the electrical offset ($EOS_{V,H}$), the linearity error and the RMS linearity error. Figure 12 displays the measured data along with linear fits

TABLE IV. Measured linearity and sensitivity parameters of the prototype stripline BPM for both high and low power test configurations in the installation with axis-oriented electrodes.

Parameter	Meas. LP	Meas. HP	Theory	Simulation
		Vertical		
S_V [m^{-1}]	103.3 ± 1.8	103.0 ± 2.3	166.67	137.01
EOS_V [mm]	-1.64 ± 0.05	-1.74 ± 0.07	0.00	0.00
σ_V [μm]	164.25	141.88		
		Horizontal		
S_H [m^{-1}]	105.8 ± 2.1	134.8 ± 4.3	166.67	137.01
EOS_H [mm]	-2.21 ± 0.06	-1.49 ± 0.08	0.00	0.00
σ_H [μm]	85.22	181.36		

As in the test of the installation with 45-rotated electrodes, the measured vertical sensitivity has been found lower than the simulated value, 103.3 m^{-1} instead of 137.01 m^{-1}. The F-type quadrupole at position 0900, between the two TBL inductive BPMs used as reference, is again thought to have an influence in the reference vertical positions read by the inductive BPM at position 0910. There are no further remarkable effects of the increase of the extracted PETS RF power on this parameter.

The measured horizontal sensitivity, however, starts with a lower value than expected in the low extracted PETS power test configuration, 105.8 m^{-1}, becoming closer, 134.8 m^{-1}, to the simulated value of 137.01 m^{-1} in the high extracted PETS power test configuration. The fluctuations of the available beam in the low extracted PETS power configuration may have resulted in non-negligible differences between the test beams used for different positions, affecting also the measured positions by the reference BPMs 0850 and 0910.

For operational aspects, it is possible to increase these sensitivities in both low and high extracted PETS power test configurations by estimating the position as a polynomial function of the difference-over-sum ratio instead of a linear one. A fifth degree polynomial fit of the measured position data for the stripline installation with axis-oriented electrodes increases all sensitivity values in Table IV by 30 m^{-1}. However, this does not eliminate the observed effects of the extracted PETS power increase in the horizontal sensitivity and provides a too high value for this parameter in the high extracted PETS power configuration.

A variation in the electrical offset was observed for the coordinate not being swept (Figure 12). In addition, for this coordinate in both the high- and low-power test configurations, a tilt was observed, of 5 mrad for the horizontal plane and 4 mrad for the vertical one.

B. Resolution

Following the sensitivity and linearity tests of the stripline BPM prototype with short-circuited electrodes, a preliminary resolution test was performed using Singular Value Decomposition (SVD) analysis. The SVD method decomposes the data, allowing to identify and separate systematic beam effects (modes), such as betatron motion, cavity phase/energy errors, RF jitter, etc. from uncorrelated statistical noise of the BPMs (BPM noise floor) and thus provide an estimate of the resolution of each BPM on the line. The use of this technique for the analysis of BPM data was first proposed in [12]. Further successful examples of its application can be found in [13] and [14].

The objective of this analysis is to estimate the resolution of the CLIC DB stripline BPM with short-circuited electrodes, based on shot-to-shot position data collected from all the 17 TBL BPMs. For this purpose, position data from 966 consecutive, synchronous shots from a 3 A beam were acquired and analysed in the stripline BPM installation with axis-oriented electrodes. Table V shows the assigned number, location and type of all TBL BPMs considered in this study, including the stripline BPM prototype.

The procedure starts by considering a B matrix of dimensions $P \times M$, where P is the number of shots and M the number of BPMs, containing the position data from all TBL BPMs, having substracted their mean values per column (orbit). This matrix can be factorized in the form:

$$B = U \cdot S \cdot V^T \tag{7}$$

where U is a $P \times P$ matrix containing the temporal eigenvectors and V is a $M \times M$ matrix containig the spatial eigenvectors. Both are orthogonal matrices. S is a $P \times M$ diagonal matrix containing non-negative values (eigenvalues or modes).

The diagonal elements of S, $s_{ii}, 1 \leq i \leq M, i \in \mathbb{N}$, normalized by $\sqrt{MP}$, give the correlation level between the U and V matrices: the larger their value, the higher the correlation. They are shown in Fig. 13 for both the horizontal and the vertical planes. It is possible to observe that the first eight elements of S have large values, accounting for correlated beam motion, while elements 9 to 17 are due to the uncorrelated BPM noise floor.

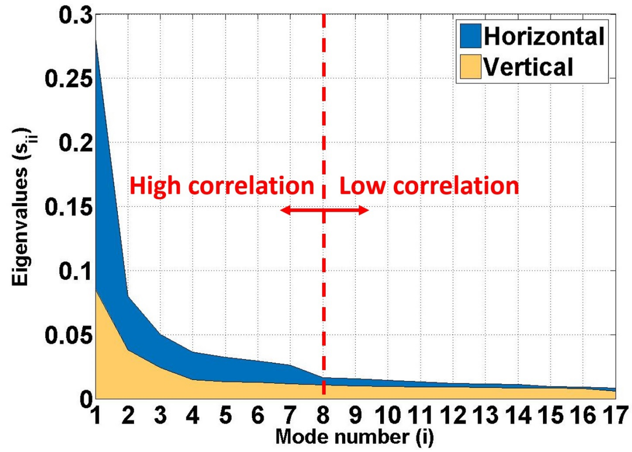

FIG. 13. Normalized diagonal elements s_{ii} of the S matrix. The first eight elements define the high correlation region due to beam motion, while the elements 9 to 17 belong to the low correlation region due to the BPM noise floor.

Setting modes 1 to 8 to zero, we obtain a new diagonal matrix S', from which it is possible to reconstruct the data matrix B' where only uncorrelated BPM noise floor is present:

$$B' = U \cdot S' \cdot V^T \tag{8}$$

TABLE V. TBL BPM locations, type and assigned numbers for the SVD analysis.

BPM number	TBL location	BPM type
1	210	Inductive
2	250	Inductive
3	310	Inductive
4	350	Inductive
5	410	Inductive
6	450	Inductive
7	510	Inductive
8	550	Inductive
9	610	Inductive
10	650	Inductive
11	710	Inductive
12	750	Inductive
13	810	Inductive
14	850	Inductive
15	860	Stripline
16	910	Inductive
17	950	Inductive

The standard deviation values $\sigma_i, i \in [1, 17], i \in \mathbb{N}$, of the columns of B' provide the resolution for all 17 BPMs (Fig. 14).

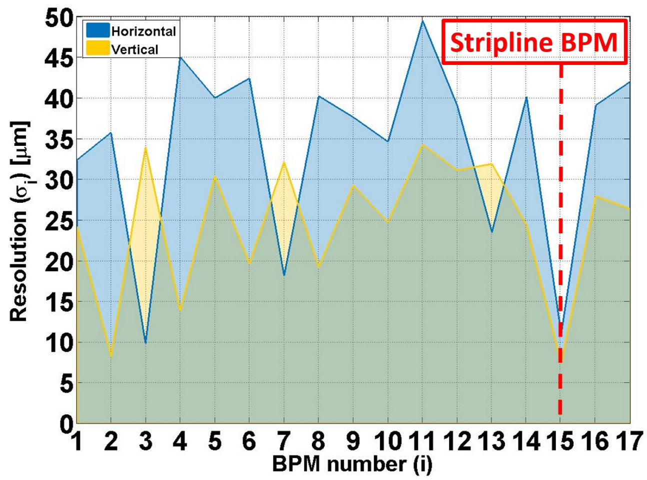

FIG. 14. Standard deviation per columns of the B' matrix, indicating the resolution of each BPM in TBL.

The preliminary estimated resolution values for the stripline prototype with short-circuited electrodes, BPM#15, are 11 μm in the horizontal plane and 7.4 μm in the vertical plane.

V. TERMINATED STRIPLINE PROTOTYPE

The compact stripline BPM prototype, as described in section III, is not providing the expected transfer response of an ideal stripline BPM. The discrepancy is particularly large at high frequencies, due to geometry constraints as described in [9], and as a result this BPM with short-circuited stripline electrodes at their downstream end provides insufficient filtering of the PETS RF power at 12 GHz. In order to improve this issue, a modified version with downstream terminated electrodes (eight ports) has been developed. It provides an improved suppression of unwanted 12 GHz RF signals, while offering a loop-through calibration with test signals using the downstream ports.

The design was revised to achieve an effective notch filter effect at 12 GHz, the frequency of the PETS RF interference. In this approach we tuned the third notch of the stripline transfer response to 12 GHz, $N = 3$ in Eq. (1), as tuning the first or the second notch results in a quite short physical length of the electrode, having a similar dimension as the beam pipe diameter, which causes unwanted resonances [9]. This choice results in an electrode length of $L = 37.5$ mm and an ideal response to a multi-bunch train (Fig. 15) that only shows the first and last triplets of bunches. The signals from all other bunches in-between will cancel, assuming the notch filter effect is perfect and precisely tuned to 12 GHz. Table VI

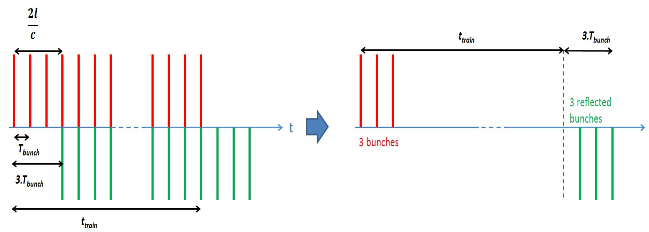

FIG. 15. Time response of the terminated prototype stripline BPM PU to a multi-bunch beam.

TABLE VI. Parameters of the compact prototype stripline BPM for the CLIC Drive Beam.

Parameter	Value	Comment
Diameter	23 mm	
Stripline length	37.5 mm	
Width	5.55 %	of circumference (20°)
Characteristic impedance	50 Ω	
Duct aperture	23 mm	
Resolution	2 μm	Full train
Accuracy	20 μm	
Time resolution	10 ns	BW > 20 MHz

shows the relevant design parameters and dimensions for this new prototype.

Similarly as in the first prototype, a ring of SiC has been placed at each end of the striplines, separated from their rounded end by a narrow gap, to damp a strong resonance peak of the transverse wake impedance observed in EM simulations around 12 GHz. However, while successfully damping higher order modes (HOMs), the dielectric ring also increases the effective electrical length of the stripline electrodes (or shifts the notches to lower frequencies). To account for this effect, the actual physical distance between the upstream and downstream port pins was reduced to 36.6 mm. The stripline electrodes of the terminated design have a smaller angular coverage (20° vs. 45°) to ensure a TEM-like field propagation, reducing unwanted spurious resonances and providing an improved transfer response. Fig. 16 shows an assembly view of the prototype. Further details of the design can be found in [15].

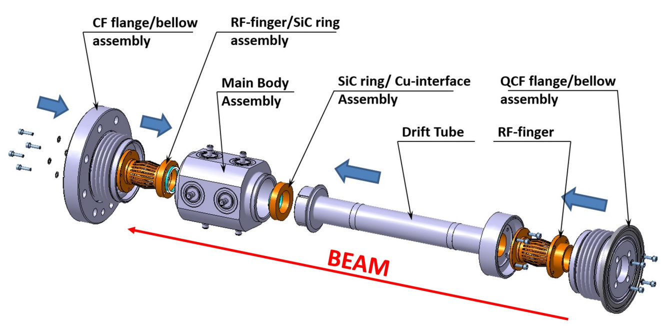

FIG. 16. Assembly view of the terminated prototype stripline BPM prototype for the CLIC Drive Beam.

In contrast to the prototype with short-circuited electrodes, the frequency response of the modified pick-up (Fig. 17) resembles that of an ideal stripline BPM up to higher frequencies ($\sim$8 GHz). An unavoidable resonance appears around 10 GHz, which seems to be caused by the TM_{01} waveguide mode of the vacuum chamber [9]. However, a substantial notch effect at 12 GHz is still present, and should improve the suppression to the PETS high power RF fields.

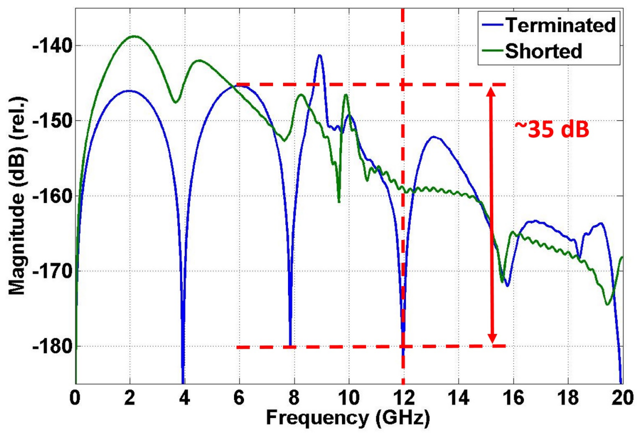

FIG. 17. Frequency responses of the compact (green trace) and terminated (blue trace) prototype stripline BPMs for the CLIC Drive Beam.

The signal processing scheme for this prototype is very similar to the one from the first design, operating at baseband frequencies, ranging from 8 to 80 MHz, to stay well separated from the microwave PETS frequency. The cut-off frequencies of the passive filtering stages have been doubled to improve the time resolution. Minor adjustments in the attenuation and gain stages of the readout electronics allow to adapt the signals produced by all possible CLIC Drive Beam configurations to the input range of the ADC. A calibrator has been included, with two operation modes: white noise or pulse train. The selected calibration signal is converted to analog and fed into the stripline electrodes through the downstream ports.

Two units of this prototype have been installed in the Drive Beam line of the CLIC Two Beam Module, in positions 0645 and 0685, and will be tested with beam in fall 2015. A preliminary test with calibration pulses has resulted in position sensitivity values around the origin of 153.0 m^{-1} (V) and 163.0 m^{-1} (H) for the BPM at position 0645 and 167.7 m^{-1} (V) and 152.5 m^{-1} (H) for the one at position 0685. These values are close the one obtained by electromagnetic simulation (Fig. 18): 155.3 m^{-1}.

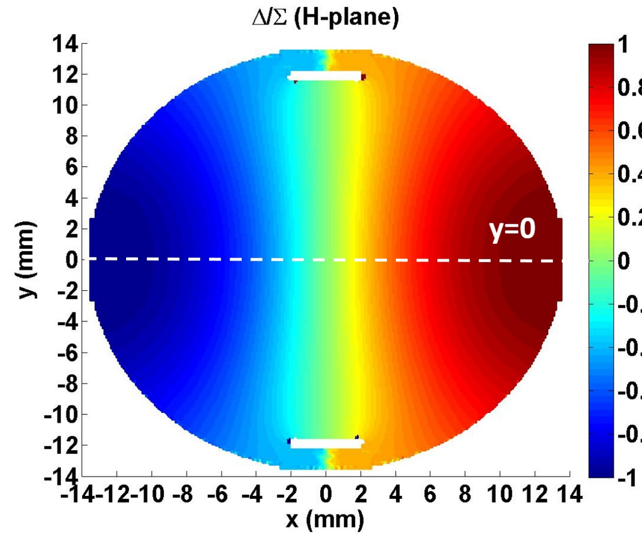

FIG. 18. Simulated difference-over-sum ratio in the cross-section of the terminated prototype stripline BPM for the horizontal plane.

VI. CONCLUSIONS

The laboratory characterization tests of the first prototype stripline BPM, both in the low and high frequency ranges, with thin wire and coaxial waveguide test bench, respectively, have been described in section III. The measured horizontal and vertical sensitivity values in the characterization tests with a thin wire (Table II), both around 115.2 m^{-1}, are closer to the simulated value (137 m^{-1}) than to the theoretically expected one using the linear approximation from Eq. (2) (166.67 m^{-1}). Charge accumulation and impedance mismatches in the measurement setup are most likely the causes of this difference in sensitivity values. The measured filtering properties of the pick-up at 12 GHz in the coaxial test bench are not as they were expected from the basic theory, and the rejection around this frequency is only about 4 dB (Fig. 8). This problem has been addressed by the development of a new stripline prototype with improved notch filter effect at 12 GHz, using the recommendations of the study performed in [9]. Additionally, using terminated electrodes instead of downstream short-circuited ones is expected to increase the tunability of the stripline frequency response notches to a given frequency, and to add a calibration functionality via the downstream port.

The influence of these observations on the performance of the BPM was further studied during the tests with beam at CTF3. In the linearity and sensitivity tests of the installation with 45°-rotated electrodes, the measured sensitivities for each plane (Table III) experience a -4% variation upon the increase of the extracted PETS RF power from 6 to 60 MW. The measured horizontal sensitivity values (98.1 m^{-1} and 94.2 m^{-1} for 6 and 60 MW, respectively) remain close to the simulated value of 101.8 m^{-1}, while the vertical sensitivity was found systematically lower (72.4 m^{-1} and 75.3 m^{-1} for 6 and 60 MW, respectively). The same effect has been observed for the vertical sensitivity for both low and high (2.4 and 27 MW) extracted PETS power test configurations for the installation with axis-oriented electrodes. The nonlinear effects can be mitigated by correcting the position characteristic of the pick-up using a higher order polynomial or a look-up table.

During the beam studies of the first prototype stripline BPM, the position data of all the TBL BPMs was analyzed applying the Singular Value Decomposition (SVD) method. This technique allowed the separation of the correlated beam motion effects and the uncorrelated BPM noise, finding an upper resolution boundary for the latter of 11 μm for the horizontal plane and 7.4 μm for the vertical one (Fig. 14). However, an improvement can be expected at higher beam currents in the TBL line of CTF3.

Two units of the terminated prototype have been installed in the Drive Beam line of the CLIC TBM and will be tested with beam in fall 2015. The results of a preliminary test with calibration signals match the simulated values for the position sensitivity.

ACKNOWLEDGMENTS

This research project has been supported by the U.S. Department of Energy under contract number DE-AC02-76SF00515 and Spain's Ministry of Economy and Competitiveness (MINECO) under contract numbers FPA2010-21456-C02-01, SEIC-2010-00028 and FPA2013-47883-C2-1-P.

[1] M. Aicheler, P. Burrows, M. Draper, T. Garvey, P. Lebrun, K. Peach, N. Phinney, H. Schmickler, D. Schulte, and N. Toge, eds., *A Multi-TeV linear collider based on CLIC technology: CLIC Conceptual Design Report*, CERN-2012-007.

[2] S. Smith, A. Capelletti, D. Gudkov, L. Søby, and I. Syratchev, in *Proceedings of the 10th European Workshop on Beam Diagnostics and Instrumentation for Particle Accelerators*, Hamburg, Germany, 2011, pp. 326–328.

[3] G. Geschonke and A. Ghigo, eds., *CTF3 Design Report*, CTF3 Note 2002-047.

[4] G. Riddone, A. Samoshkin, and D. Gudkov, in *Proceedings of the 2010 Linear Accelerator Conference*, Tsukuba, Japan, 2010, pp. 91–93.

[5] A. Samoshkin, D. Gudkov, A. Solodko, and G. Riddone, in *Proceedings of the 2nd International Particle Accelerator Conference*, San Sebastián, Spain, 2011, pp. 1003–1005.

[6] A. Benot-Morell, A. Faus-Golfe, J. García-Garrigós, J. Nappa, S. Smith, L. Søby, J. Tassan-Viol, and S. Vilalte, in *Proceedings of the 3rd International Particle Accelerator Conference*, New Orleans, USA, 2012, pp. 873–875.

[7] R. E. Shafer, in *AIP Conference Proceedings*, Vol. 212 (1989) pp. 26–58.

[8] J. J. García-Garrigós, C. Blanch-Gutiérrez, J. V. Civera-Navarrete, A. Faus-Golfe, and B. Gimeno-Martínez, in *Proceedings of the 10th European Workshop on Beam Diagnostics and Instrumentation for Particle Accelerators*, Hamburg, Germany, 2011, pp. 335–337.

[9] A. Benot-Morell, J. Nappa, S. Smith, L. Søby, J. Tassan-Viol, S. Vilalte, and M. Wendt, in *Proceedings of the 1st International Beam Instrumentation Conference*, Tsukuba, Japan, 2012, pp. 87–89.

[10] S. Doebert, D. Schulte, and I. Syratchev, *Status Report of the CTF3 Test Beam Line*, CTF3-Note-076.

[11] J. J. García-Garrigós, *Development of the Beam Position Monitors for the Diagnostics of the Test Beam Line in the CTF3 at CERN*, PhD dissertation, Polytechnic University of Valencia, Department of Electronic Engineering (2013).

[12] C. X. Wang, *Model Independent Analysis of Beam Centroid Dynamics in Accelerators*, PhD dissertation, Stanford University, Department of Applied Physics (1999).

[13] C. Wang, M. Borland, K. Kim, and V. Sajaev, in *Proceedings of the 2001 Particle Accelerator Conference*, Chicago, USA, 2001, pp. 1354–1356.

[14] J. Tan, M. Ludwig, M. Sordet, L. Søby, and M. Wendt, in *Proceedings of the 4th International Particle Accelerator Conference*, Shanghai, China, 2013, pp. 750–752.

[15] A. Benot-Morell, A. Faus-Golfe, J. Nappa, S. Smith, L. Søby, S. Vilalte, and M. Wendt, in *Proceedings of the 2nd International Beam Instrumentation Conference*, Oxford, UK, 2013, pp. 384–387.